

# Culture of Tumorigenic Cells on Protein Fibers Reveals Metastatic **Cell Behaviors**

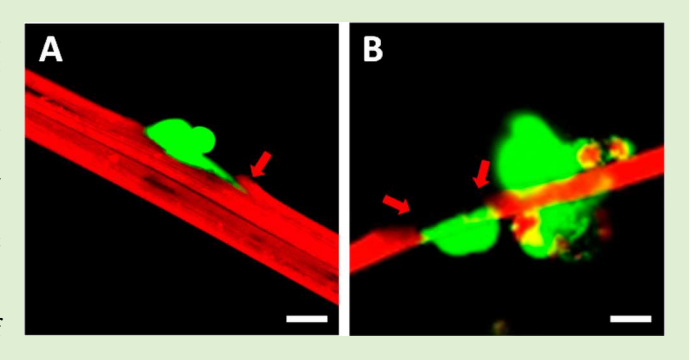
Hao-Ching Hsiao, Andres Santos, David W. Howell, Jan L. Patterson, Robin S.L. Fuchs-Young, and Sarah E. Bondos\*

Department of Molecular and Cellular Medicine, Texas A&M University Health Science Center, College Station, Texas 77843, United States

Department of Biosciences, Rice University, Houston Texas 77251, United States

Supporting Information

ABSTRACT: Tumorigenic cell behaviors can be suppressed or enhanced by their physicochemical environment. As a first step toward developing materials that allow tumorigenic behaviors to be observed and manipulated, we cultured related MCF10 breast cell lines on fibers composed of the Drosophila protein Ultrabithorax (Ubx). These cell lines, originally derived from fibrocystic breast tissue, represent a continuum of tumorigenic behavior. Immortal but nontumorigenic MCF10A cells, as well as semitumorigenic MCF10AT cells, attached and spread on Ubx fibers. MCF10CA-1a cells, the most highly transformed line, secreted high concentrations of matrix metalloproteinases when cultured on Ubx materials,



resulting in differences in cell attachment and cytoskeletal structure, and enabling invasive behavior. Because the mechanical and functional properties of Ubx fibers can be genetically manipulated, these materials provide a valuable tool for cancer research, allowing creation of diverse microenvironments that allow assessment of invasive, metastatic behavior.

## ■ INTRODUCTION

Because cell culture is versatile, rapid, and cost-effective, it has been widely used for basic research and preclinical studies. Although the cellular environment in vivo is composed of threedimensional (3D) elements, 1,2 most cells are cultured on a twodimensional (2D) surface. For cancer cells, culture on a 2D surface can suppress the behaviors that characterize the level of transformation and invasive phenotype. 3-8 For instance, matrix metalloproteinases (MMPs) are required for cell extravasation during metastasis and, thus, serve as a prognostic for a high recurrence rate and poor survival. 9-11 In vitro, expression of MMPs is downregulated when cells are cultured on a 2D flat surface relative to a 3D scaffold composed of the same materials.<sup>12</sup> Furthermore, the combination of mechanical and topological cues provided by the substrate can combine to influence cancer cell behavior in important, yet unexpected ways. 8,13,14 For instance, cancer cells are more resistant to anticancer drugs on a 3D substrate than a 2D substrate. 15

An ideal cell culture substrate would (i) replicate the chemistry and topology of the tumor microenvironment, (ii) allow facile control of structural and mechanical properties, (iii) display or deliver cell binding and bioactive molecules, and (iv) enable observation of tumorigenic behaviors. Combined, these characteristics accommodate multiple experimental designs and facilitate investigations of tumorigenic cell behavior in response to a variety of external cues. Many natural and chemically synthesized materials have been adapted from tissue engineering to establish 3D cancer cell culture systems in vitro.  $^{8,19-22}$ Difficulties in optimizing the properties of the materials for cancer cell culture and incorporating bioactive molecules result in few materials meeting all of the above requirements.<sup>23–27</sup>

Materials composed of the Drosophila melanogaster Ultrabithorax (Ubx) protein have the potential to solve this problem. In vivo, Ubx monomers function as transcription factors. <sup>28,29</sup> In vitro, Ubx self-assembles into nanoscale to macroscale materials that can be easily manipulated to form multiple complex 3D structures. 30,31 Ubx fibers and fiber bundles mimic the size and topology of aligned, dense collagen fibrils, which are components of the extracellular matrix important for invasion. <sup>32–34</sup> In addition, since Ubx materials are composed of amino acids, which are a natural component of extracellular matrix proteins, they meet the first criterion of similar chemistry. Ubx fibers also have mechanical properties comparable to elastin, and these properties can be further optimized by genetically altering dityrosine bond content, fulfilling the second criterion. Finally, Ubx fibers can be readily functionalized and patterned with a wide variety of active peptides and proteins via gene fusion, the third criterion. 30,37

In this study, we specifically examined the ability of Ubx materials to meet the forth criterion: to support and enable

Received: September 1, 2016 Published: September 21, 2016

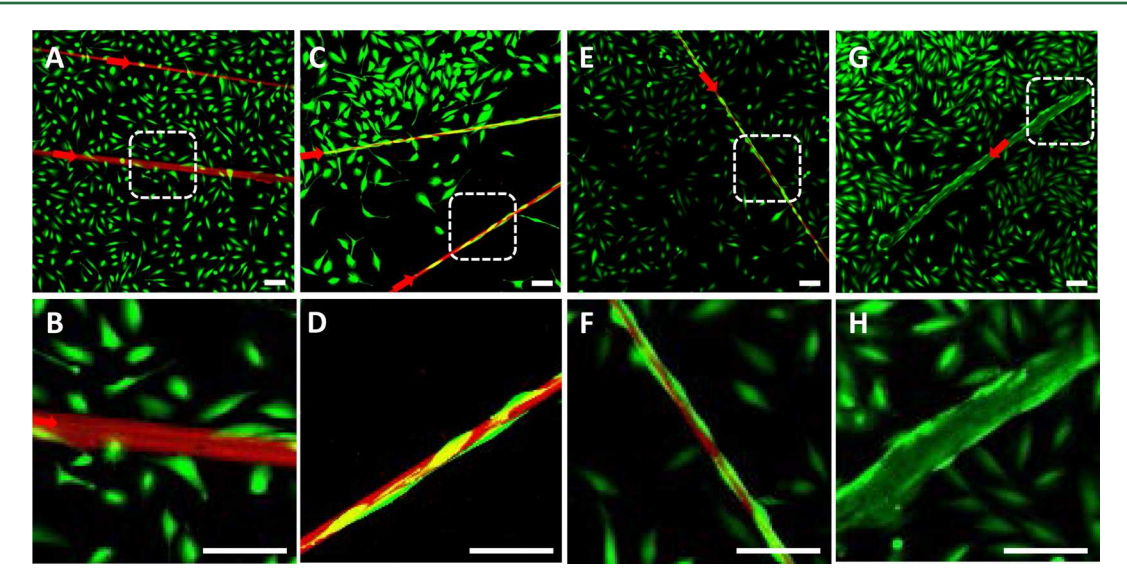


Figure 1. Ubx fibers are not toxic to MCF10A cells. Live/dead cell viability assays demonstrate the viability of MCF10A cells at 6 (A,B), 12 (C,D), 24 (E,F), and 48 h (G,H), respectively. Red arrows indicate the position of Ubx fibers, which stain red. Live MCF10A cells stain green and dead cells stain red in this assay. White dashed rectangles indicate the area enlarged for panels B, D, F, and H. Scale bars equal 100  $\mu$ m.

observation of tumorigenic cell behaviors in culture. The first step is to determine whether Ubx materials are compatible with culture of three different cell lines representing a continuum of phenotypic transformation. Importantly, immortal but non-tumorigenic cells readily adhere to Ubx materials, which can serve as a nontoxic and nonimmunogenic substrate for cell culture. Assessing the cytocompatibility of Ubx materials with more tumorigenic cells is particularly relevant because a portion of the Ubx amino acid sequence is identical to the peptide penetratin, a member of a family of positively charged peptides that can penetrate and kill cancer cells.

To determine whether the level of transformation of cells affects cell compatibility with Ubx materials, we used three related human breast cell lines with varying abilities to form tumors in nude/immunocompromised mice: MCF10A, MCF10AT, and MCF10CA-1a. The MCF10A cell line was derived from a benign fibrocystic lesion and is nontumorigenic. The premalignant MCF10AT cell line, generated by transforming MCF10A cells with the T24 c-Ha-ras oncogene, forms relatively indolent and noninvasive tumors in nude mice. Finally, the MCF10CA-1a cell line, derived through serial xenografts of MCF10AT cells, is a highly transformed cell line with strong metastatic potential.

Because the MCF10 cell lines are derived from a single source, they provide an opportunity for determining how transformation impacts cell behavior while minimizing other variables. We assessed how culture on Ubx materials impacts cell morphology, cell adhesion, cytoskeletal structure, and scaffold proteolysis. Our results suggest that Ubx materials facilitate the analysis and manipulation of metastatic behaviors, with the largest effects observed in the most tumorigenic cells.

# **■ EXPERIMENTAL SECTION**

**Ubxla Protein Expression and Purification.** His-tagged Ultrabithorax Ia protein (Ubx) was expressed as previously described.  $^{30,38,39,46}$  In brief, the pET19b-UbxIa plasmid was transformed into the BL21(DE3)-pLysS strain of *Escherichia coli* (EMD Millipore). UbxIa protein expression was induced by adding 1 mM isopropyl β-D-1-thiogalactopyranoside (IPTG) at the log phase of growth (optical density at 600 nm = 0.65–0.7),

followed by incubation at 25 °C for 2 h with shaking at 200 rpm. Cells were harvested by centrifugation for 5 min at 1200g at 4 °C. Cell pellets, in aliquots corresponding to 2 L of bacterial culture, were stored at −20 °C in 5 mL of phosphate buffered saline (80 mM Na<sub>2</sub>HPO<sub>4</sub>, 20 mM NaH<sub>2</sub>PO<sub>4</sub>, and 100 mM NaCl at pH 7.4). A frozen cell pellet was lysed in 15 mL of lysis buffer, which contains 50 mM  $NaH_2PO_4$  (pH = 8.0), 5% glucose (w/v), and 500 mM NaCl (Buffer G) with one ethylenediaminetetraacetic acid-free protease inhibitor tablet (Roche), and 1.2 mg/L DNase I. After centrifugation at 10 000g for 30 min at 4 °C, the supernatant was incubated with Ni-NTA resin (Thermo Scientific) pre-equilibrated with Buffer G for 15 min prior to pouring the column. The column was iteratively washed with 10 column volumes of Buffer G containing 20 mM, 40 mM, and 80 mM imidazole followed by elution of Ubx in 10 mL Buffer G containing 200 mM imidazole. Purified, monomeric Ubx was stored at 4 °C until use for Ubx fiber production.

Production of Ubx Fibers and Bundles. Ubx protein fibers were generated using the buffer reservoir system as previously described.<sup>46</sup> Fiber diameters ranged from 20 to 40  $\mu$ m. To provide support for Ubx bundles, 10  $\mu$ L plastic inoculation loops (VWR) were placed in ZipLoc plastic bags and flattened with a hammer. Following UV sterilization for 15 min on each side, the flattened loops were used to draw fibers from a tray, wrapping the fibers around the loops. To fuse recently produced Ubx fibers into bundles, fiber-wrapped flattened loops were rested on a sterile surface. Buffer G was applied to the inoculation loops to cover Ubx fibers with a thin layer of liquid. Buffer G was slowly removed by pipetting from the area between the Ubx fibers and the inside edge of inoculation loops, thus forcing the Ubx fibers into contact and forming Ubx bundles (Supporting Information, Figure 1). The Ubx bundles were dried in a biosafety cabinet for 30 min before placement onto the sterile chamber slides (Ibidi).

**Cell Culture.** All cell lines were obtained from the repository at the Barbara Ann Karmanos Cancer Institute. MCF10A and MCF10AT cells were cultured in sterile DMEM/F12 media containing 0.12% sodium bicarbonate (w/v) (Sigma), 5% heat inactivated fetal bovine serum (w/v) (FBS,

Gibco), 10  $\mu$ g/mL insulin (Sigma), 20 ng/mL epidermal growth factor (Gibco), 0.5  $\mu$ g/mL hydrocortisone (Life Technologies), 15 mM 4-(2-hydroxyethyl)-1-piperazineethane-sulfonic acid (HEPES, Caisson), and 17.5 mM glucose at pH = 7.4, at 5% CO<sub>2</sub> and 37 °C. MCF10CA-1a cells were cultured in DMEM/F12 media containing 0.12% sodium bicarbonate (w/v), 10% horse serum (w/v) (Gibco), 15 mM HEPES (Caisson), and 17.5 mM glucose at pH = 7.4, at 5% CO<sub>2</sub> and 37 °C. Inoculation loops, each wrapped multiple times with a single Ubx fiber, were placed in separate wells on the chamber slide, and 20 000–30 000 cells were cultured inside each loop for the times specified.

Immunostaining. A freshly made 8% paraformaldehyde (w/v) stock in Dulbecco's phosphate-buffered saline (DPBS, Life Technologies) was added to the existing culture media at a final concentration of 4%, and samples were fixed at room temperature for 2 h. Fixed samples were washed three times for 10 min with 200  $\mu$ L wash buffer 1 (25 mM Tris, 200 mM glycine). Samples were permeabilized with 200  $\mu$ L of DPBS containing 0.5% Triton X-100 (Sigma) for 20 min at room temperature. Wells were aspirated, and 300 µL of blocking solution containing 0.1% Triton X-100, 1% bovine serum albumin (BSA, Sigma) and 5% goat serum was added for 1 h at room temperature. Following removal of the blocking solution, samples were washed three times for 10 min each with Wash Buffer 2 (0.1% Triton X-100 in DPBS) and then incubated in 100  $\mu$ L of anti  $\alpha$ -tubulin antibodies (Sigma), diluted 1:50 in blocking solution, and incubated for 1 h at room temperature. Samples were washed three times for 10 min each in 200  $\mu$ L of Wash Buffer 2, and incubated with a 1:200 dilution of goat antimouse Alexa 488 conjugated secondary antibody (Life Technologies) in blocking solution for 30 min at room temperature. Finally, samples were washed 3 times in 300  $\mu$ L DPBS containing 0.1% Triton X-100 prior to incubation for 10 min in 10  $\mu$ M of 4',6-diamidino-2-phenylindole (DAPI, Molecular Probes) and imaging on a Nikon Eclipse Ti confocal microscope equipped with NIS Elements AR 4.10.01 software. Each cell line/time point combination was measured at least 3 times, with a minimum of three replicates in each experiment.

**Live/Dead Cell Viability Assay.** After incubating cells with Ubx fibers for the times specified, the media was aspirated and the wells were rinsed six times with 200  $\mu$ L of DPBS containing 0.05 mM Mn<sup>2+</sup> and 0.5 mM Mg<sup>2+</sup> to remove serum. DPBS solution (100  $\mu$ L) containing 2  $\mu$ M calcein acetoxymethylester and 4  $\mu$ M ethidium homodimer-1 (Live/dead viability/cytotoxicity kit for mammalian cells, Molecular Probes) was then added into the wells for cell staining. The reagents were incubated with cells for 10 min at room temperature and imaged using confocal and fluorescent microscopy on a Nikon Eclipse Ti confocal microscope equipped with NIS Elements AR 4.10.01 software. Images were acquired in differential interference contrast (DIC) or fluorescence format. Each cell line/time point combination was measured at least three times, with a minimum of three replicates in each experiment.

Matrix Metalloproteinases (MMPs) Target Sites Prediction. The locations of MMP target sites on the Ubx Ia protein sequence were predicted using the PROSPER program (https://prosper.erc.monash.edu.au/downloads.html).<sup>47</sup>

**Proteolysis Inhibition Assay.** In the wells of a chamber slide, 200  $\mu$ L of media containing approximately 20 000 MCF10CA-1a cells were seeded in loops supporting Ubx bundles. The broad spectrum MMP inhibitor GM6001 (Santa Cruz Biotechnology) was serially diluted in DPBS and added

into media, yielding a final concentration of 12  $\mu$ M. The total number of intact Ubx fibers was recorded immediately after the initial seeding of MCF10CA-1a cells. An individual Ubx fiber lacking any internal breakpoints and connected on both ends to the inoculation loop was considered an intact fiber. The percentage of intact Ubx fibers at each designated time point divided by total the number of intact Ubx fibers at the initial time point was calculated for each sample. Experiments were repeated three times. The total number of fibers tested in each condition is given in the figure legends.

In Vitro MMP9 Activity Experiment. The design of the MMP9 digestion experiment was similar to trypsin digestion of Ubx fibers described in a previous study. <sup>39</sup> Ubx fibers were wrapped around a plastic inoculation loop, air-dried for 2 h in a biosafety cabinet for 30 min, and then placed in a chamber slide. MMP9 (Sino Biological Inc.) was diluted to  $100 \, \mu \text{g/mL}$  then activated by incubation with 1 mM p-aminophenylmercuric acetate (APMA) dissolved in MMP Assay Buffer (50 mM Tris, 10 mM CaCl<sub>2</sub>, 150 mM NaCl, 0.05% (w/v) Brij35 (Life Technologies) at pH 7.5) for 24 h at 37 °C. Activated MMP9 was further diluted to  $40 \, \mu \text{g/mL}$  in Assay Buffer before application to Ubx fibers in the chamber slide. Ubx fibers were visualized by confocal microscopy on a Nikon Eclipse Ti equipped with NIS Elements AR 4.10.01 software.

## ■ RESULTS AND DISCUSSION

Ubx materials are engineerable, functionalizable, and mimic the properties of the extracellular matrix. These materials provide a convenient tool for studying how environmental cues impact cell responses and tumorigenic behavior. Previous studies in our laboratory have shown that plain Ubx and mCherry-Ubx protein fusion materials are nontoxic and allow growth of several primary human cell lines. However, the Ubx protein sequence includes the sequence of penetratin, which belongs to a family of cell-penetrating peptides with antimicrobial and/or anticancer properties. To determine whether Ubx materials can serve as a nontoxic substrate for cancer cell culture, we monitored both cell attachment and cell viability over time for three MCF10 cell lines.

Ubx Fibers Are Compatible with MCF10A Cells. MCF10A cells, which are an immortalized, nontransformed breast epithelial line,  $^{43}$  were seeded in a chamber slide containing culture medium and Ubx fibers. Cell attachment and viability were determined by live/dead cell viability stains that were visualized using confocal and fluorescence microscopy at 6, 12, 24, and 48 h. No evidence of cell death was observed for MCF10A cells in contact or close proximity (<10  $\mu \rm m$ ) to Ubx fibers, demonstrating that Ubx materials are not toxic to these cells (Figure 1E,F,G,H). Furthermore, cells far from Ubx fibers (>10  $\mu \rm m$ ) also survive, demonstrating that Ubx materials also do not secrete substances into the media that are toxic to MCF10A cells.

Interestingly, once bound to the fiber, MCF10A cells often elongate along the fiber axis. A similar phenomenon has previously been observed for MCF10A cells bound to aligned poly-L-lactic acid fibers. Since the chemical nature of poly-L-lactic acid and Ubx protein are substantially different, the fibrous topology of the substrate appears to elicit the observed change in cell shape. After 48 h of culture, the axial alignment of MCF10A cells was still apparent, although the cells had spread to completely cover the fiber (Figure 1G,H).

Ubx Materials Are Compatible with MCF10AT Cells. The above experiments were repeated with MCF10AT cells,

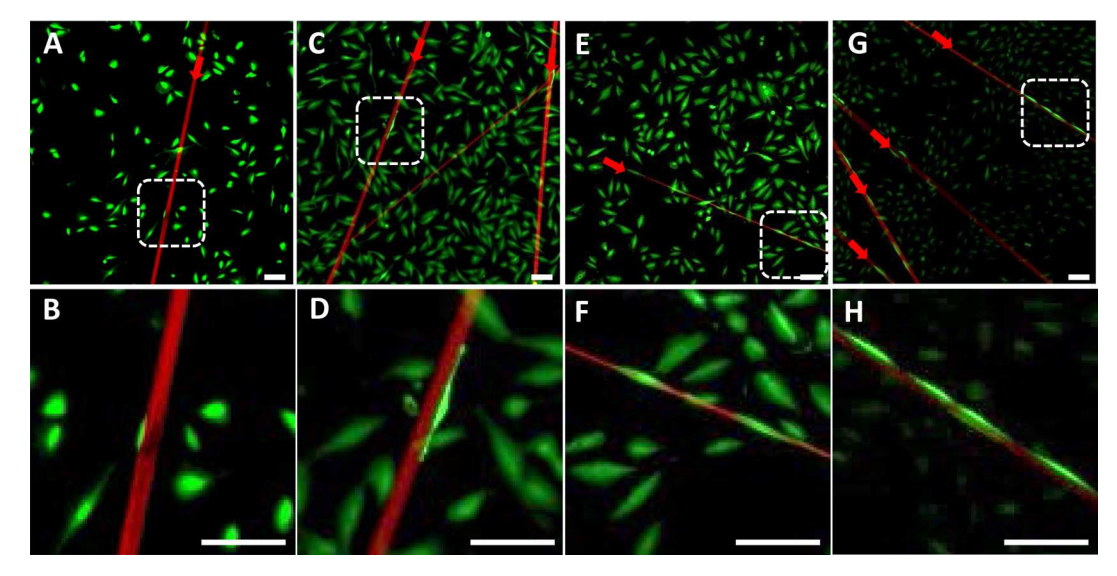


**Figure 2.** Ubx fibers are not toxic to MCF10AT cells. Live/dead cell viability assays were performed to test the viability of MCF10AT cells at 6 (A,B), 12 (C,D), 24 (E,F), and 48 h (G,H), respectively. Images are marked as in Figure 1. Scale bars equal 100  $\mu$ m for panels in the top row and 10  $\mu$ m in panels on the bottom row.

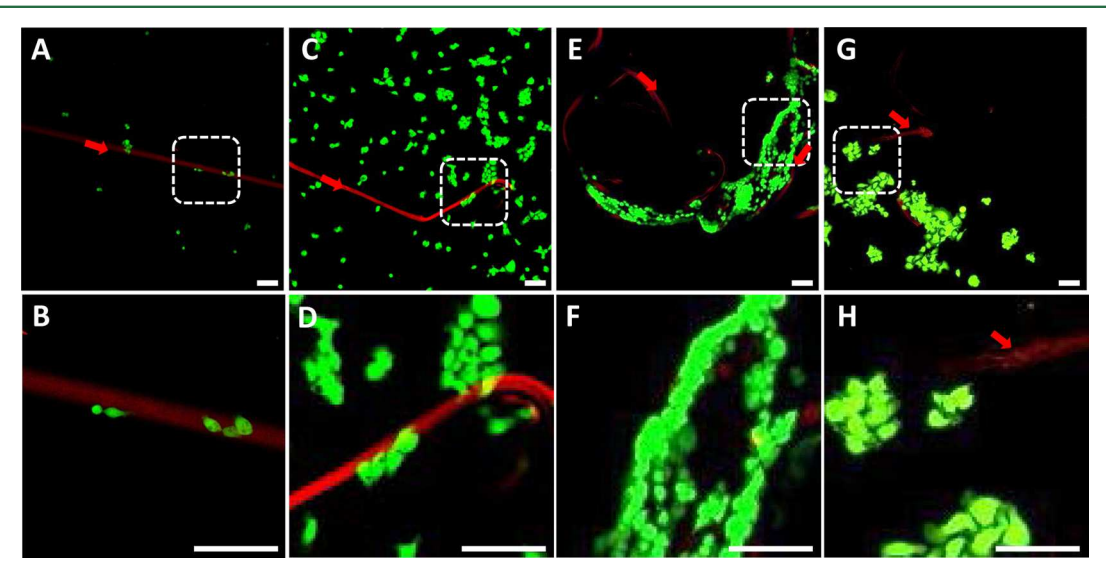


Figure 3. Ubx fibers are not toxic to MCF10CA-1a cells. Live/dead cell viability assays demonstrate MCF10CA-1a cells are viable on Ubx materials for 6 (A,B), 12 (C,D), 24 (E,F), and 48 h (G,H), respectively. Images are marked as in Figure 1. Scale bars represent 100  $\mu$ m.

which are considered semitumorigenic because they will form slow growing tumors that rarely invade surrounding tissue in immunocompromised mice. Ho signs of cell death were observed when MCF10AT cells were incubated with Ubx fibers at 6, 12, 24, or 48 h (Figure 2). These results indicate that the Ubx fibers are similarly nontoxic to MCF10AT cells, and do not secrete overtly toxic substances. Although cell attachment improved with time, MCF10AT cells did not reach confluency on Ubx fibers within 48 h, as observed for the MCF10A when seeded at a similar density (Figure 2). These differences in attachment may reflect differences in cell growth rates.

Unlike MCF10A cells, single, attached MCF10AT cells were frequently observed on the sides (Figure 2 B,D) of Ubx fibers. Furthermore, MCF10AT cells appeared to attach more rapidly, visibly aligning with the axis of Ubx fibers after only 6 h. These phenomena may reflect the increased capacity of MCF10AT cells for migration, or increased attachment of MCF10AT cells to Ubx fibers, relative to MCF10A cells. As observed with the

MCF10A cells, all MCF10AT cells attached to Ubx fibers were often elongated. We conclude that Ubx fibers are compatible with both MCF10A and MCF10AT cells, which represent immortal, but untransformed and nontumorigenic cells, and immortal and modestly tumorigenic mammary cells, respectively, in the series.

Ubx Fibers Are Compatible with, but Degraded by, MCF10CA-1a Cells. The Ubx protein sequence includes the sequence of the penetratin peptide which can bind, penetrate, and even kill cancer cells. This peptide was originally isolated from the third helix of the DNA-binding domain of Antennapedia, another *Drosophila* Hox transcription factor. The Ubx and Antennapedia sequences are identical in this region. Therefore, viability of MCF10CA-1a cells, the most tumorigenic cell line tested, on Ubx fibers was of particular interest. Although physical attachment of live MCF10CA-1a cells was observed at 6 and 12 h (Figure 3A,B,C,D), no signs of cell death were observed for MCF10CA-1a cells that are either

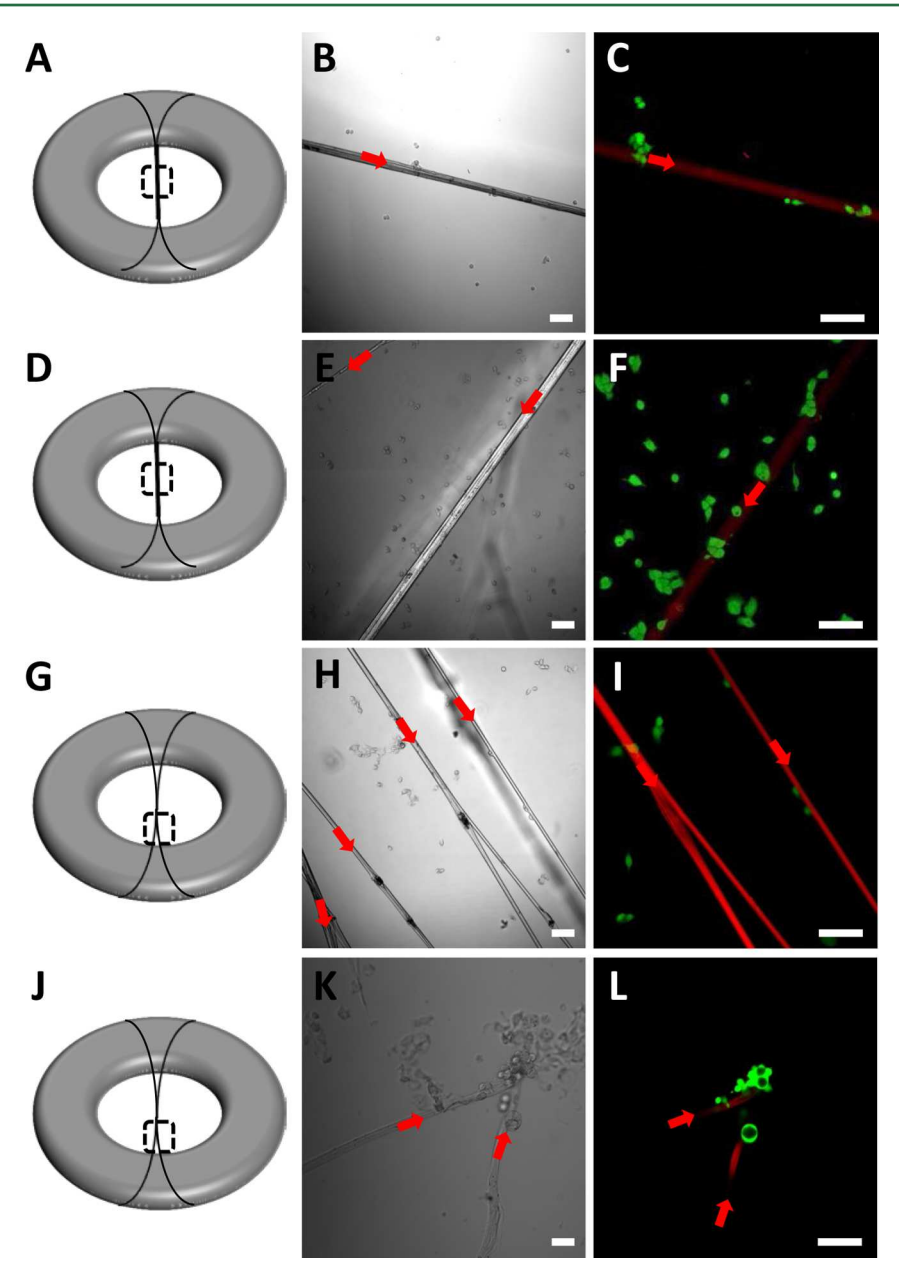


Figure 4. MCF10CA-1a cells can be cultured for longer times on Ubx bundles. (A,D,G,J) Schematics of Ubx bundles supported by flattened inoculation loops. The structure of bundles is different in the center of the bundle (completely fused) versus at the edge of the bundle (Y shaped). The position of confocal images to the right is indicated by black dashed rectangles on each schematic. Before live/dead staining, DIC images were taken at 6 (B), 12 (E), 24 (H), and 48 (K) hours after the initial seeding to show the relative position and cell population at different time points. After live/dead viability assays, fluorescence microscopy was used to assess the viability of cells at the same locations. The bends, caused by a lack of tension in the bundles shown in panels K and L, indicate that the bundles, although largely intact, have been severed at least once. Red arrows indicate Ubx bundles. Scale bars indicate  $100 \ \mu m$  in all panels.

in direct contact with or in close proximity to Ubx fibers (Figure 3). Therefore, penetratin, as a component of solid materials, does not exhibit antitumorigenic properties during short-term culture.

Following 6 h of incubation with MCF10CA-1a cells, many Ubx fibers had ruptured. After 24 h of culture, MCF10CA-1a cells covered much of the surface of the remaining materials. However, by this point the fibers were severely damaged and sheared into thin fragments that were difficult to visualize microscopically (Figure 3E,F). Within 48 h of incubation, virtually all Ubx fibers were in fragments  $10-20~\mu m$  in size (Figure 3G,H). Additional time was required to rupture Ubx fibers with larger diameters. To further assess this, we created

Ubx bundles in which multiple fibers were fused in parallel, to generate wider diameters (Supporting Information, Figure S1),<sup>30</sup> thus potentially enhancing the durability of the materials. As expected, the Ubx bundles were largely intact at 6, 12, and 24 h, although they began to break at 48 h, indicated by both visible ruptures as well as slack or bending in the bundles, reflecting a reduction of tension (Figure 4). No signs of cell death were observed during this time frame.

The delayed degradation of Ubx materials provided a valuable opportunity to monitor the behavior of MCF10CA-1a cells over extended incubation times. Although the surface topography of cell culture substrates can affect cell growth and viability, <sup>49,50</sup> the change in the topography caused by

substituting Ubx bundles for fibers did not alter the viability of the MCF10CA-1a cells. There was no sign of increased cell death of MCF10CA-1a cells at any time point or location (Figure 4C,F,I,L). Therefore, Ubx materials are suitable for creating a multidimensional cancer cell scaffold in culture systems. Similarly, antibacterial peptides fused to silk proteins killed bacteria as monomers, but not when assembled into silk materials.<sup>51</sup> Given this class of peptides is expected to kill cells by associating to create pores, 52 the spacing of the peptide imposed by monomer packing in materials may preclude pore formation, and hence toxicity. Alternately, in Ubx materials, covalent intermolecular interactions involving other regions of the DNA-binding domain, combined with the stability of the DNA binding domain, may prevent the penetratin sequence from dissociating from this domain and interacting to form pores.

Only MCF10CA-1a cells were capable of breaking Ubx fibers and bundles, regardless of the size of the bundle (Figure 4). To determine how MCF10CA-1a cells rupture Ubx fibers, we compared images taken at different time points. At 6 h, individual MCF10CA-1a cells were observed near areas where Ubx fibers were partially destroyed (Figure 5A), but fibers

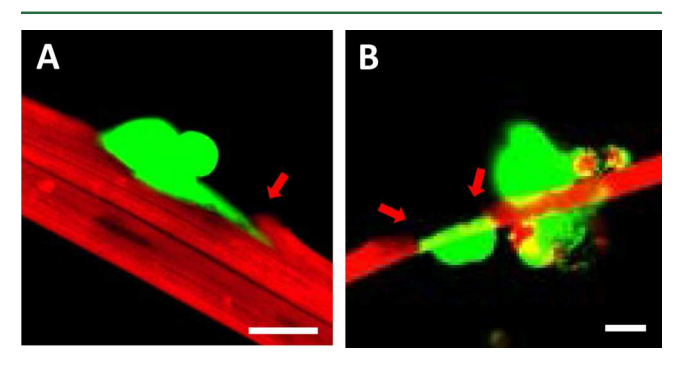


**Figure 5.** Proteolysis of Ubx fibers by MCF10CA-1a cells. (A) MCF10CA-1a cells (green) situated on a partially destroyed (red arrow) Ubx fiber (red linear structure) at 6 h after the initial seeding. (B) MCF10CA-1a cells (green) situated on a Ubx fiber (red linear structure) at 12 h after the initial seeding. Ubx fibers were proteolyzed to a greater extent (red arrows). Scale bars equal 10  $\mu$ m in all panels.

remained intact in the areas devoid of the MCF10CA-1a cells. Staining studies revealed that the MCF10CA-1a cells were capable of invading the fibers to form a wedge-shaped, lacunalike gap in the fibers that strongly resembles metastatic bone lesions (Figure 5A). Because fibers form by collapsing and folding the film layers during fiber "drawing", the interface between layers may be weaker and thus more susceptible to proteolysis and invasion. Indeed, application of force to rupture the fiber can cause the outer layers of the fiber to peel away from the core, also suggesting the interface between layers may be weaker in fibers. After 12 h of culturing with MCF10CA-1a cells, the observed damage to Ubx fibers was extensive, with portions of the fibers appearing to be completely dissolved (Figure 5B).

Although all MCF10 cell lines tested were able to spread when cultured on tissue culture plastic, culture on Ubx fibers revealed notable differences in cell behavior and morphology. MCF10A and MCF10AT cells attached and initially spread along the fiber axis, before extending laterally around the fiber. By contrast, MCF10CA-1a cells consistently exhibited a rounded phenotype. This difference in cell morphology suggests that MCF10CA-1a cells may not adhere as well to

Ubx fibers. Indeed, changes in cell adhesion and cell spreading have previously been correlated with increased proteolysis in A2058 cells. These data, combined with the degradation of Ubx fibers by the MCF10CA-1a cell lines, suggest that changes in the levels of proteases secreted by these cell lines are responsible for the differences in the morphology of cells cultured on Ubx fibers. Indeed, degradation of the extracellular matrix and consequent loss of adherence is required for tumor cell invasion and migration. S4

**Cytoskeletal Structures Mirror Differences in Cell Adhesion and Topology.** To determine the extent to which changes in the morphology of these cells extended to differences in cytoskeletal organization, we immunostained MCF10 cells for  $\alpha$ -tubulin. The orientation of microtubules in MCF10A cells cultured on tissue culture plastic aligned with the major cell axis, with a few protrusions, presumably involved in cell attachment, extending along the minor cell axis after 48 h of culture, at which time MCF10A cells are well spread on both tissue culture plastic and Ubx fibers (Figure 6). Although the  $\alpha$ -

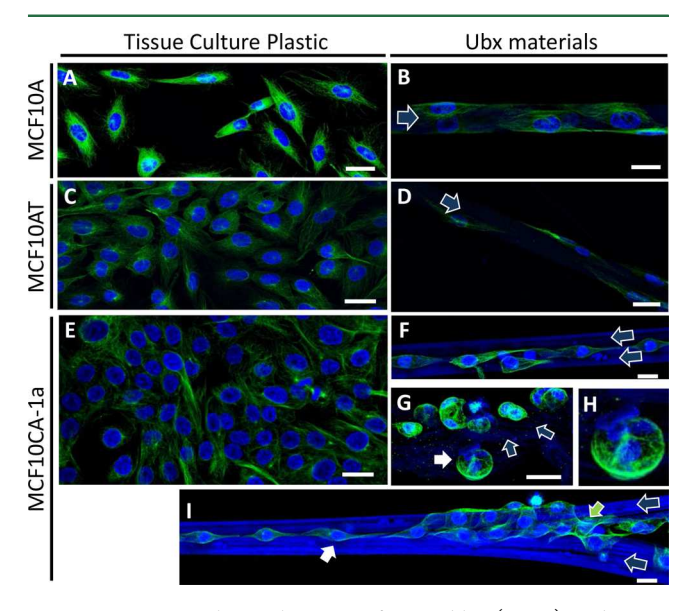


**Figure 6.** Immunochemical staining for  $\alpha$ -tublin (green) and DAPI stained nuclei (blue) reveal differences in cytoskeletal organization among MCF10 cell lines and in the same cell line cultured on Ubx materials versus tissue culture plastic. (A) MCF10A cells cultured on tissue culture plastic. (B) MCF10A cells cultured on Ubx fibers. (C) MCF10AT cells cultured on tissue culture plastic. (D) MCF10AT cells cultured on the Ubx fibers (blue arrows). (E) MCF10CA-1a cells cultured on tissue culture plastic. (F) MCF10CA-1a cells cultured on intact Ubx fibers (blue arrows). (G) MCF10CA-1a cells, bound to a broken Ubx fiber segment (blue arrows) that has been flayed open, either have divided nuclei or form small clusters of cells (white solid arrow and panel H). (I) MCF10CA-1a cells preferentially bind the groove between multiple fibers (white arrow) and the junction between multiple fibers (green arrow). A four-fiber bundle is shown. All images were collected 48 h after seeding cells. Scale bars equal 10  $\mu$ m in all panels.

tubulin of MCF10A cells cultured on Ubx fibers also aligned with the major cell axis (and the Ubx fiber axis), protrusions were observed along minor axis of the cells. For MCF10AT cells on tissue culture plastic, the cytoskeletal structures were more heterogeneous, sometimes extending radially from the nucleus, compared to the tight  $\alpha$ -tubulin alignment frequently observed for MCF10AT cells cultured on Ubx fibers. The differences in observed microtubule structures correlated with

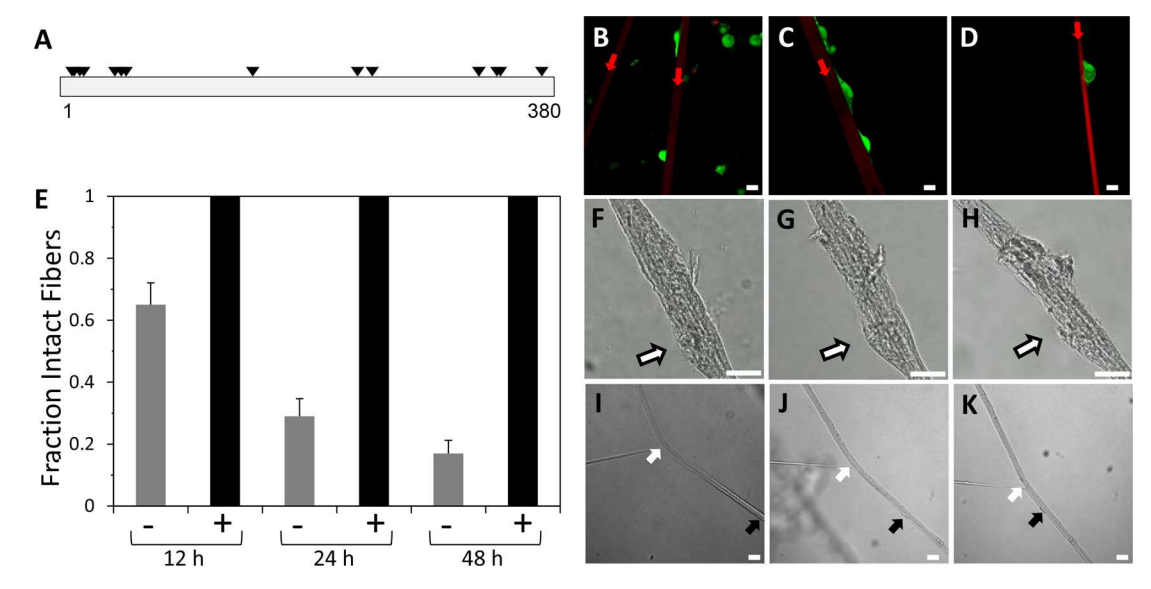


Figure 7. MMPs are required for destruction of Ubx fibers by MCF10CA-1a cells. (A) A schematic of the Ubx protein sequence, with locations of MMP9 cleavage sites predicted using PROSPER are marked with black arrow heads. <sup>47</sup> In the presence of 12  $\mu$ M of the broad spectrum MMP inhibitor GM6001, MCF10CA-1a cells remain alive and do not proteolyze Ubx fibers after (B) 12 h, (C) 24 h, or (D) 48 h in culture. (E) Time course experiments with GM6001 show inhibition of Ubx fiber destruction by MCF10CA-1a cells. The "+" and "-" symbols indicate data collected with and without the addition of the MMP inhibitor, GM6001, respectively. For the 12 and 24 h samples, n = 8. For the 48 h data, n = 7. (F–K) DIC images of Ubx fibers (F–H) and a Ubx bundle of fibers (I–K) incubated with 40  $\mu$ g/mL MMP9 for 0 (F, I), 12 (G, J), and 36 h (H, K), respectively. (F–H) MMP9 exposure narrows Ubx fibers and causes lesions to form (white arrows in F–H). MMP9 exposure also dissociates a Ubx bundle. Black arrows indicate a thicker portion of the Ubx fibers which serves as a visual reference point, whereas white arrows mark the junction between the two fibers, which moves as the fibers separate. Scale bars equal 10  $\mu$ m in all panels with microscopy images.

the differences in MCF10AT cell structure, and did not appear to be strongly influenced by the substrate on which the cells were cultured.

Dramatic  $\alpha$ -tubulin rearrangements were observed for MCF10CA-1a cells cultured on Ubx materials (Figure 6E,F,G). On tissue culture plastic, the tubulin structures in MCF10CA-1a cells extended across the entire cell. In contrast, the MCF10CA-1a cells lodged between Ubx fibers had a large aspect ratio, and  $\alpha$ -tubulin in these cells aligned with the cell/ bundle axis (Figure 6F). MCF10CA-1a cells on broken Ubx fibers had either divided nuclei or formed cell clusters and were significantly more compact (rounded up) than MCF10CA-1a cells cultured either on tissue culture plastic or intact Ubx fibers. In these rounded cells,  $\alpha$ -tubulin was located in a dense ring surrounding the nucleus (Figure 6G). This  $\alpha$ -tubulin distribution resembled that of cells grown in the presence of apple polyphenol, which suppresses cell attachment. 55 Likewise, tubulin disruption, which yields similar cell structures, is linked with decreased cell attachment in mice. 56

Because MCF10CA-1a cells take longer to rupture the thicker fiber bundles, these structures remain under tension for longer times. When cultured on Ubx fiber bundles, MCF10CA-1a cells preferentially bind the grooves formed at the interface between multiple fibers, where they are better able to elongate (Figure 6F, I). In contrast, MCF10CA-1a cells that bind at the junction between multiple fibers spread in multiple directions (Figure 6I). In both cases, MCF10CA-1a cells cultured on bundles appear more like those cultured on tissue culture plastic. However, cells on bundles still do not spread or elongate to the extent observed on tissue culture plastic, and tubulin was still more dense at the cell periphery. Although cytoskeletal differences between the MCF10 cell lines were not apparent on tissue culture plastic, substantial differences,

correlating with the tumorigenicity of the cell line, were apparent when cells were cultured on Ubx fibers.

Importantly, the differences in MCF10CA-1a cell morphology on fiber fragments, bundle grooves, and bundle junctions demonstrate that these cells actively respond to the three-dimensional topology of the fiber bundles. Because different basic forms of Ubx materials, such as fibers and film, readily meld to form stable, complex structures including baskets and meshes, <sup>30</sup> Ubx materials present an opportunity to explore the behavior of MCF10CA cells in a wide variety of three-dimensional environments.

Destruction of Ubx fibers by MCF10CA-1a cells is type-specific and requires Matrix Metalloproteinases (MMPs). Metastasis is the process by which tumor cells break away from the primary tumor and travel to and colonize at distant sites<sup>57</sup> and is a fundamental characteristic of cancer.<sup>5</sup> Metastasis is a complex, multistep cascade that involves acquisition of a morphologic and biochemical phenotype that permits invasion of cancer cells across the basement membrane and into local tissues. Metastatic cells also must also acquire the ability to survive in the circulatory or lymphatic systems and to again invade tissue and proliferate at distant sites. There is substantial literature on the molecular, genetic, and cellular mechanisms that contribute to the metastatic phenotype. Despite this complexity, several paradigms emerge. Genes that promote metastasis include those that (1) stimulate mitosis and proliferation, such as members of oncogenic growth factor signaling systems; (2) inhibit apoptosis and enhance cell survival; and (3) enhance invasion, including increased production of tissue proteases, pro-inflammatory molecules, and cell motility proteins.

Matrix metalloproteineases (MMPs) are a family of endopeptidases that can degrade most extracellular matrix proteins. These proteases facilitate tissue invasion and meta-

stasis of solid malignant tumors.<sup>59</sup> MMP-2 and -9, in particular, have been shown to have important roles in metastasis of breast and hepatocellular carcinomas.<sup>60</sup> Overexpression of these proteases is associated with increased risk of relapse, metastasis, invasion, progression, and reduced overall survival.

Metastatic cancer cells often express high level of proteases during invasion, a trait that has been observed in 3D cell culture. 61–63 In particular, MMPs are upregulated in the more tumorigenic MCF10CA cells, compared with nontumorigenic MCF10As, 64,65 suggesting that secreted MMPs are a possible mediator of the observed fiber damage. Indeed, the PROSPER program identified multiple potential MMP cleavage sites in the Ubx sequence (Figure 7A). Many of the predicted MMP9 cleavage sites are in intrinsically disordered (unstructured) regions of the Ubx protein, that have been previously demonstrated to be accessible to proteases in Ubx monomers. 66

To investigate this possibility, we cultured MCF10CA-1a cells on Ubx fibers in the presence of the broad spectrum MMP inhibitor, GM6001. If MMPs are responsible for proteolyzing Ubx fibers, then GM6001 should inhibit this activity. In the presence of GM6001, MCF10CA-1a cells did not damage Ubx fibers, although fibers from the same preparation were readily cleaved by MCF10CA-1a cells in the absence of GM6001 (Figure 7A-D). Cell viability assays confirmed that MCF10CA-1a cells cultured on Ubx fibers remained viable in the presence of GM6001 (Figure 7A-C), demonstrating that GM6001 did not inhibit fiber damage by inducing cell death. GM6001 had no effect on the culture of MCF10A cells on Ubx fibers, and induced MCF10AT cells to form small, granular shapes both on tissue culture plastic and on Ubx fibers (Figure 2 in the Supporting Information). Therefore, the ability of MG6001 to induce MCF10CA-1a cells to spread out, rather than round up, on Ubx fibers is specific to that cell line. We conclude that MMPs, overexpressed by MCF10CA-1a cells, are necessary for destruction of Ubx fibers. The rapid speed with which fibers were degraded also suggests that MCF10CA-1a cells recognize Ubx fibers as a 3D substrate, and thus secrete high levels of MMPs. By contrast, previous reports indicate that growth on 2D substrates down-regulates MMP expression. 12

MMPs are a large family of degradative enzymes including collagenases, gelatinases, stromelysins, and the membrane-type MMPs. To verify that metalloproteinases can damage Ubx fibers, we added purified MMP9 to Ubx fibers. MMP9 was selected because the PROSPER program identified multiple MMP9 proteolysis cutting sites within the Ubx protein sequence (Figure 7A). Although we added very high concentrations of purified MMP9 to the reaction, the maximum possible concentration was still more than an order of magnitude less than the concentration of trypsin required to rupture fibers.<sup>39</sup> Ubx fibers were visibly damaged by MMP9 exposure (Figure 7F-H): fibers became narrower, and small fragments of the fibers were partially separated. Furthermore, although Ubx bundles are stable in solution,<sup>38</sup> purified MMP9 can dissociate (unzip) Ubx bundles (Figure 7I-K). Thus, MMPs are both necessary (inhibitor experiments) and sufficient (MMP9 proteolysis) to damage Ubx materials. We conclude that MMPs, secreted by MCF10CA-1a cells, are a major contributor to the destruction of Ubx fibers.

The fact that the cells are able to digest Ubx fibers so quickly is particuly noteworthy given that (i) MMP cut sites occur less frequently in the Ubx protein sequence than they do in extracellular matrix proteins such as collagen, (ii) extremely high concentrations of trypsin are required to rupture Ubx

fibers, <sup>30</sup> and (iii) Ubx monomers are covalently cross-linked in Ubx fibers, resulting in a mechanical strength comparable to elastin<sup>35</sup> and exceeding collagen.<sup>67</sup> Some portion of the difference in cleavage rates can likely be attributed to the intrinsically disordered nature of much of the Ubx protein versus the highly ordered structure of collagen.<sup>68</sup> Even so, the rapid proteolysis of Ubx fibers is a reflection of the extraordinarily high concentrations and/or complexity of proteases secreted by MCF10CA-1a cells. Thus, the use of these Ubx fibers allows assessment of extracellular matrix proteolysis by tumorigenic cells, a critical step in cancer invasion (Figure 8).<sup>61,69</sup>

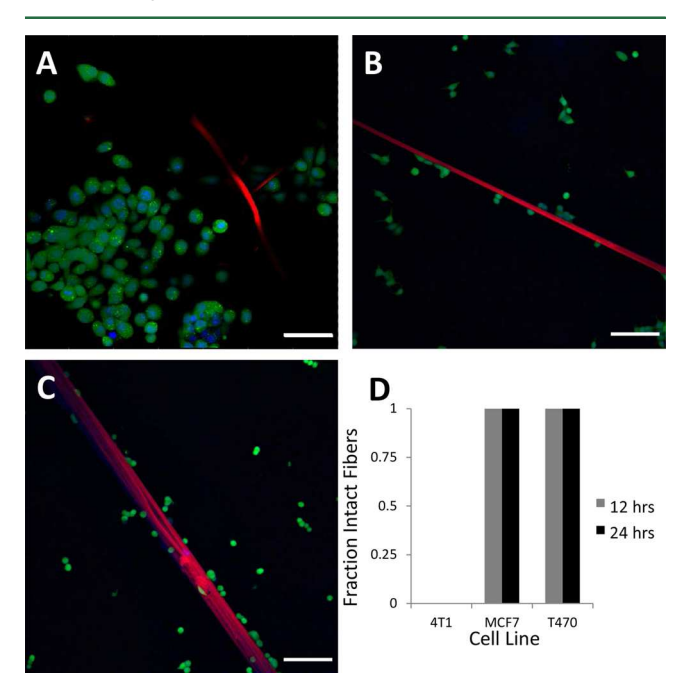


**Figure 8.** Rupture of Ubx fibers correlates with metastatic potential in other cancer cell lines. (A) 4T1 cells rupture mCherry-Ubx fibers (red). Tubulin is immunostained green, and nuclei are stained blue by DAPI. In contrast, MCF-7 (B) and T47D (C) cells bind, but do not proteolyze, Ubx fibers. (D) Quantitation of fiber proteolysis by the three cell lines after 12 h of culture (n=8) and 24 h (n-13). Scale bars represent 50  $\mu$ m.

The Ability of Other Cell Lines to Rupture Ubx Fibers Correlates with Metastatic Potential. If the ability of MSCF10CA-1a cells to proteolyze and degrade Ubx materials reflects invasive potential, and is not a quirk unique to this cell line, then other invasive cell lines should display this behavior. To test this hypothesis, we examined the ability of three additional cell lines derived from mammary tumors. Although all three cell lines are categorized as metastatic, MCF-7 and T47D cells rarely metastasize when grafted into nude mice without either genetic manipulation or providing supplemental estrogen. 70-72 By contrast, 4T1 cells, like MCF10CA-1a cells, readily metastasize when grafted in vivo. The 4T1 cell line was able to proteolyze Ubx fibers at a remarkably rapid rate; all fibers were ruptured after only 12 h of culture. Although MCF-7 and T47D cells could clearly bind Ubx fibers, they were unable to rupture these materials within 24 h. Therefore, the ability to proteolyze Ubx fibers correlates with the metastatic potential of the cells. Overexpression of proteases by cancer cells is associated with increased risk of relapse, metastasis, invasion, progression, and reduced overall survival.

#### CONCLUSION

In this study, we demonstrated that materials composed of Ubx protein provide three-dimensional scaffolds and are useful for characterizing the metastatic activities of immortal and transformed cells. Despite the presence of an antitumorigenic peptide in the Ubx sequence, Ubx materials are compatible with all MCF10 breast cell lines tested, regardless of the degree of transformation.

Culture of MCF10 breast cell lines on Ubx materials allow observation of metastatic behaviors that arise *in vivo*, but are not evident in cultures on tissue culture plastic. Differences in cytoskeletal structure between the three cell lines were observed on Ubx materials but not tissue culture plastic. In particular,  $\alpha$ -tubulin in MCF10CA-1a cells formed a dense ring at the cell periphery, characteristic of decreased cell attachment. These differences in cell shape and organization reflected cell-line specific changes in attachment and adaptation to the 3D environment.

MMPs, secreted by MCF10CA-1a cells, proteolyzed Ubx fibers at a remarkable rate. The half-life of a fiber on which MCF10CA-1a cells were cultured was between 12 and 24 h, with more than one-third of fibers ruptured after only 6 h exposure. By comparison, incubation of Ubx fibers with 40  $\mu$ g/mL MMP9 for 36 h damaged, but failed to rupture, Ubx fibers. While incubation of Ubx fibers with 2 mg/mL trypsin for 15 h created more extensive damage, again the fibers were not completely ruptured. Furthermore, all fibers in culture with the highly metastatic 4T1 cells ruptured in 12 h. These comparisons speak to the extremely high concentrations of proteases secreted by tumorigenic cells. By contrast, MCF10A, MCF10AT, MCF7, or T47D cells did not proteolyze Ubx fibers; thus, this effect is a metastatic cell behavior.

Overall, our results demonstrate the potential of using Ubx materials to establish *in vitro* 3D cell culture for characterization of cancer cell invasion and metastasis. In the long term, the mechanical, functional, and genetic properties of Ubx materials can be easily manipulated to study invasion and protease production at different stages of tumor progression, invasion, and metastasis, and the effects of potential therapeutic approaches on these characteristics.

# ASSOCIATED CONTENT

#### **S** Supporting Information

The Supporting Information is available free of charge on the ACS Publications website at DOI: 10.1021/acs.bio-mac.6b01311.

A detailed description of producing Ubx bundles, and the effect of the MMP-inhibitor GM6001 on MCF10A and MCF10AT cells (PDF)

### AUTHOR INFORMATION

## **Corresponding Author**

\*E-mail: SEBondos@medicine.tamhsc.edu; phone: 979-436-0807; fax: 979-847-9481.

#### **Author Contributions**

H.C.H., A.S., D.H., and J.L.P. performed experiments. The manuscript was drafted by HCH and edited by all authors. All authors have given approval to the final version of the manuscript.

# Notes

The authors declare no competing financial interest.

#### ACKNOWLEDGMENTS

Funding was provided by NSF CAREER 1151394, the Ted Nash Long Life Foundation M1500779, and the TAMHSC RDEAP to S.E.B. The authors would especially like to thank Shang-Pu Tsai, and other members of the Bondos and Fuchs-Young laboratories for helpful discussions.

#### ABBREVIATIONS

BSA,bovine serum albumin; DAPI,6-diamidino-2-phenylindole; DIC,differential interference contrast; DPBS,Dulbecco's phosphate-buffered saline; HEPES,of 4-(2-hydroxyethyl)-1-piperazineethanesulfonic acid; MMP,matrix metalloproteinase; Ubx,Ultrabithorax

#### REFERENCES

- (1) Cukierman, E.; Pankov, R.; Stevens, D. R.; Yamada, K. M. Science **2001**, 294, 1708–1712.
- (2) Yamada, K. M.; Cukierman, E. Cell 2007, 130, 601-610.
- (3) Ziolkowska, K.; Kwapiszewski, R.; Brzozka, Z. New J. Chem. 2011, 35, 979-990.
- (4) Pampaloni, F.; Reynaud, E.; Stelzer, E. H. K. Nat. Rev. Mol. Cell Biol. 2007, 8, 839-845.
- (5) Delcommenne, M.; Streuli, C. H. J. Biol. Chem. 1995, 270, 26794–26801.
- (6) Ghosh, S.; Spagnoli, G.; Martin, I.; Ploegert, S.; Demougin, P.; Heberer, M.; Reschner, A. J. Cell. Physiol. 2005, 204, 522–531.
- (7) Talukdar, S.; Mandal, M.; Hutmacher, D. W.; Russell, P. J.; Soekmadji, C.; Kundu, S. C. *Biomaterials* **2011**, *32*, 2149–2159.
- (8) McLane, J. S.; Rivet, C. J.; Gilbert, R. J.; Ligon, L. A. Acta Biomater. 2014, 10, 4811–4821.
- (9) Sun, D. W.; Zhang, Y. Y.; Qi, Y.; Zhou, X. T.; Lv, G. Y. Cancer Epidemiol. 2015, 39, 135–142.
- (10) Galliera, E.; Tacchini, L.; Corsi Romanelli, M. M. Clin. Chem. Lab. Med. 2015, 53, 349-355.
- (11) Wolf, K.; Wu, Y. I.; Liu, Y.; Geiger, J.; Tam, E.; Overall, C.; Stack, M. S.; Friedl, P. *Nat. Cell Biol.* **2007**, *9*, 893–904.
- (12) Mishra, D.; Sakamoto, J.; Thrall, M.; Baird, B.; Blackmon, S.; Ferrari, M.; Kurie, J.; Kim, M. PLoS One 2012, 7, e45308.
- (13) Levental, K. R.; Yu, H.; Kass, L.; Lakins, J. N.; Egeblad, M.; Erler, J. T.; Fong, S. F.; Csiszar, K.; Giaccia, A.; Weninger, W.; Yamauchi, M.; Gasser, D. L.; Weaver, V. M. Cell 2009, 139, 891–906.
- (14) Baker, E. L.; Lu, J.; Yu, D.; Bonnecaze, R. T.; Zaman, M. H. *Biophys. J.* **2010**, *99*, 2048–2057.
- (15) Yamaguchi, Y.; Deng, D. W.; Sato, Y.; Hou, Y. T.; Watanabe, R.; Sasaki, K.; Kawabe, M.; Hirano, E.; Morinaga, T. *Anticancer Res.* **2013**, 33, 5301–5309.
- (16) Dunne, L. W.; Huang, Z.; Meng, W. X.; Fan, X. J.; Zhang, N. Y.; Zhang, Q. X.; An, Z. G. *Biomaterials* **2014**, *35*, 4940–4949.
- (17) Girard, Y. K.; Wang, C. Y.; Ravi, S.; Howell, M. C.; Mallela, J.; Alibrahim, M.; Green, R.; Hellermann, G.; Mohapatra, S. S.; Mohapatra, S. PLoS One 2013, 8, e75345.
- (18) Loessner, D.; Stok, K.; Lutolf, M.; Hutmacher, D.; Clements, J.; Rizzi, S. *Biomaterials* **2010**, *31*, 8494–8506.
- (19) Feng, X.; Tonnesen, M. G.; Mousa, S. A.; Clark, R. A. F. Int. J.Cell Biol. 2013, 11, 231279.
- (20) Liu, J.; Tan, Y.; Zhang, H.; Zhang, Y.; Xu, P.; Chen, J.; Poh, Y.-C.; Tang, K.; Wang, N.; Huang, B. Nat. Mater. **2012**, 11, 734–741.
- (21) Cross, V.; Zheng, Y.; Won Choi, N.; Verbridge, S.; Sutermaster, B.; Bonassar, L.; Fischbach, C.; Stroock, A. *Biomaterials* **2010**, *31*, 8596–8607.
- (22) Sieh, S.; Taubenberger, A.; Rizzi, S.; Sadowski, M.; Lehman, M.; Rockstroh, A.; An, J.; Clements, J.; Nelson, C.; Hutmacher, D. *PLoS One* **2012**, *7*, e40217.
- (23) Gelain, F.; Horii, A.; Zhang, S. G. Macromol. Biosci. 2007, 7, 544-551.
- (24) Kenney, R. M.; Boyce, M. W.; Truong, A. S.; Bagnell, C. R.; Lockett, M. R. *Analyst* **2016**, *141*, *661*.

(25) Berens, E. B.; Holy, J. M.; Riegel, A. T.; Wellstein, A. J. Visualized Exp. 2015, 105, e53409.

- (26) Alemany-Ribes, M.; Semino, C. E. Adv. Drug Delivery Rev. 2014, 79–80, 40–49.
- (27) Sharma, A.; Sharma, N. L.; Lavy, C. B.; Kiltie, A. E.; Hamdy, F. C.; Czernuszka, J. *J. Mater. Sci.* **2014**, *49*, 5809–5820.
- (28) Lewis, E. B. Nature 1978, 276, 565-570.
- (29) Appel, B.; Sakonju, S. EMBO J. 1993, 12, 1099-1109.
- (30) Greer, A. M.; Huang, Z.; Oriakhi, A.; Lu, Y.; Lou, J.; Matthews, K. S.; Bondos, S. E. *Biomacromolecules* **2009**, *10*, 829–837.
- (31) Majithia, R.; Patterson, J.; Bondos, S. E.; Meissner, K. E. Biomacromolecules 2011, 12, 3629–3637.
- (32) Conklin, M. W.; Eickhoff, J. C.; Riching, K. M.; Pehlke, C. A.; Eliceiri, K. W.; Provenzano, P. P.; Friedl, A.; Keely, P. J. *Am. J. Pathol.* **2011**, *178*, 1221–1232.
- (33) Provenzano, P. P.; Inman, D. R.; Eliceiri, K. W.; Knittel, J. G.; Yan, L.; Rueden, C. T.; White, J. G.; Keely, P. J. *BMC Med.* **2008**, *6*, 11.
- (34) Provenzano, P. P.; Eliceiri, K. W.; Campbell, J. M.; Inman, D. R.; White, J. G.; Keely, P. J. *BMC Med.* **2006**, *4*, 38.
- (35) Huang, Z.; Lu, Y.; Majithia, R.; Shah, J.; Meissner, K.; Matthews, K. S.; Bondos, S. E.; Lou, J. Biomacromolecules 2010, 11, 3644–3651.
- (36) Howell, D. W.; Tsai, S. P.; Churion, K.; Patterson, J.; Abbey, C.; Atkinson, J. T.; Porterpan, D.; You, Y. H.; Meissner, K. E.; Bayless, K. J.; Bondos, S. E. *Adv. Funct. Mater.* **2015**, 25, 5988–5998.
- (37) Tsai, S.-P.; Howell, D. W.; Huang, Z.; Hsiao, H.-C.; Lu, Y.; Matthews, K. S.; Lou, J.; Bondos, S. E. *Adv. Funct. Mater.* **2015**, 25, 1442–1450.
- (38) Patterson, J. L.; Abbey, C. A.; Bayless, K. J.; Bondos, S. E. J. Biomed. Mater. Res., Part A 2014, 102, 97-104.
- (39) Patterson, J. L.; Arenas-Gamboa, A. M.; Wang, T.-Y.; Hsiao, H.-C.; Howell, D. W.; Pellois, J.-P.; Rice-Ficht, A.; Bondos, S. E. *J. Biomed. Mater. Res., Part A* **2015**, *103*, 1546–1553.
- (40) Derossi, D.; Calvet, S.; Trembleau, A.; Brunissen, A.; Chassaing, G.; Prochiantz, A. *J. Biol. Chem.* **1996**, *271*, 18188–18193.
- (41) Jobin, M. L.; Bonnafous, P.; Temsamani, H.; Dole, F.; Grélard, A.; Dufourc, E. J.; Alves, I. D. Biochim. Biophys. Acta, Biomembr. 2013, 1828, 1457–1470.
- (42) Mader, J. S.; Hoskin, D. W. Expert Opin. Invest. Drugs 2006, 15, 933–946.
- (43) Soule, H. D.; Maloney, T. M.; Wolman, S. R.; Peterson, W. D.; Brenz, R.; McGrath, C. M.; Russo, J.; Pauley, R. J.; Jones, R. F.; Brooks, S. C. *Cancer Res.* **1990**, *50*, 6075–6086.
- (44) Dawson, P. J.; Wolman, S. R.; Tait, L.; Heppner, G. H.; Miller, F. R. Am. J. Pathol. 1996, 148, 313-319.
- (45) Santner, S. J.; Dawson, P. J.; Tait, L.; Soule, H. D.; Eliason, J.; Mohamed, A. N.; Wolman, S. R.; Heppner, G. H.; Miller, F. R. *Breast Cancer Res. Treat.* **2001**, *65*, 101–110.
- (46) Huang, Z.; Salim, T.; Brawley, A.; Patterson, J.; Matthews, K.; Bondos, S. Adv. Funct. Mater. 2011, 21, 2633–2640.
- (47) Song, J.; Tan, H.; Perry, A. J.; Akutsu, T.; Webb, G. I.; Whisstock, J. C.; Pike, R. N. *PLoS One* **2012**, *7*, e50300.
- (48) Derossi, D.; Chassaing, G.; Prochiantz, A. Trends Cell Biol. 1998, 8, 84–87.
- (49) Zheng, J.; Li, D.; Yuan, L.; Liu, X.; Chen, H. ACS Appl. Mater. Interfaces 2013, 5, 5882–5887.
- (50) Spedden, E.; Wiens, M. R.; Demirel, M. C.; Staii, C. *PLoS One* **2014**, *9*, e106709.
- (51) Gomes, S. C.; Leonor, I. B.; Mano, J. F.; Reis, R. L.; Kaplan, D. L. *Biomaterials* **2011**, 32, 4255–4266.
- (52) Kwon, B.; Waring, A. J.; Hong, M. Biophys. J. **2013**, 105, 2333—2342.
- (53) Ray, J. M.; Stetler-Stevenson, W. G. EMBO J. 1995, 14, 908–917.
- (54) Friedl, P.; Wolf, K. Nat. Rev. Cancer 2003, 3, 362-374.
- (55) Hung, C. H.; Huang, C. C.; Hsu, L. S.; Kao, S. H.; Wang, C. J. J. Funct. Foods **2015**, *12*, 80–91.
- (56) Korb, T.; Schlüter, K.; Enns, A.; Spiegel, H. U.; Senninger, N.; Nicolson, G. L.; Haier, J. Exp. Cell Res. 2004, 299, 236–247.

- (57) Liu, W.; Vivian, C. J.; Brinker, A. E.; Hampton, K. R.; Lianidou, E.; Welch, D. R. Cancer Microenviron. 2014, 7, 117–131.
- (58) Brown, G. T.; Murray, G. I. J. Pathol. 2015, 237, 273-281.
- (59) Zhang, X.; Huang, S.; Guo, J.; Zhou, L.; You, L.; Zhang, T.; Zhao, Y. Int. J. Oncol. 2016, 48, 1783–1793.
- (60) Daniele, A.; Abbate, I.; Oakley, C.; Casamassima, P.; Savino, E.; Casamassima, A.; Sciortino, G.; Fazio, V.; Gadaleta-Caldarola, G.; Catino, A.; Giotta, F.; De Luca, R.; Divella, R. *Int. J. Biochem. Cell Biol.* **2016**, *77*, 91–101.
- (61) Kessenbrock, K.; Plaks, V.; Werb, Z. Cell 2010, 141, 52-67.
- (62) Bogenrieder, T.; Herlyn, M. Oncogene 2003, 22, 6524-6536.
- (63) Shiomi, T.; Okada, Y. Cancer Metastasis Rev. 2003, 22, 145-152.
- (64) Marella, N.; Malyavantham, K.; Wang, J.; Matsui, S.-i.; Liang, P.; Berezney, R. Cancer Res. **2009**, *69*, 5946–5953.
- (65) Mbeunkui, F.; Metge, B.; Shevde, L.; Pannell, L. *J. Proteome Res.* **2007**, *6*, 2993–3002.
- (66) Liu, Y.; Matthews, K.; Bondos, S. J. Biol. Chem. 2008, 283, 20874–20887.
- (67) Miyazaki, H.; Hayashi, K. Biomed. Microdevices 1999, 2, 151–157.
- (68) Perumal, S.; Antipova, O.; Orgel, J. P. R. O. *Proc. Natl. Acad. Sci. U. S. A.* **2008**, *105*, 2824–2829.
- (69) Hanahan, D.; Weinberg, R. A. Cell 2011, 144, 646-674.
- (70) Clarke, R. Breast Cancer Res. Treat. 1996, 39, 69-86.
- (71) Zhang, H. T.; Craft, P.; Scott, P. A.; Ziche, M.; Weich, H. A.; Harris, A. L.; Bicknell, R. *J. Natl. Cancer. Inst.* **1995**, 87, 213–219.
- (72) Mattila, M. M.; Ruohola, J. K.; Karpanen, T.; Jackson, D. G.; Alitalo, K.; Härkönen, P. L. *Int. J. Cancer* **2002**, *98*, 946–951.

# **Supporting Information**

**Figure 1. Production of Ubx bundles.** Ubx bundle production process. (a) Ubx fibers (black lines) were attached to the plastic loop (grey oval shape object). Buffer G (light grey) was applied on the plastic loop with Ubx fibers using pipette (grey triangle). (b) Buffer G was removed by pipetting on both sides of Ubx fibers, forcing the two Ubx fibers to extend toward the middle, where Buffer G remains. (c) Several Ubx fibers fused to form a bundle after the removal of Buffer G.

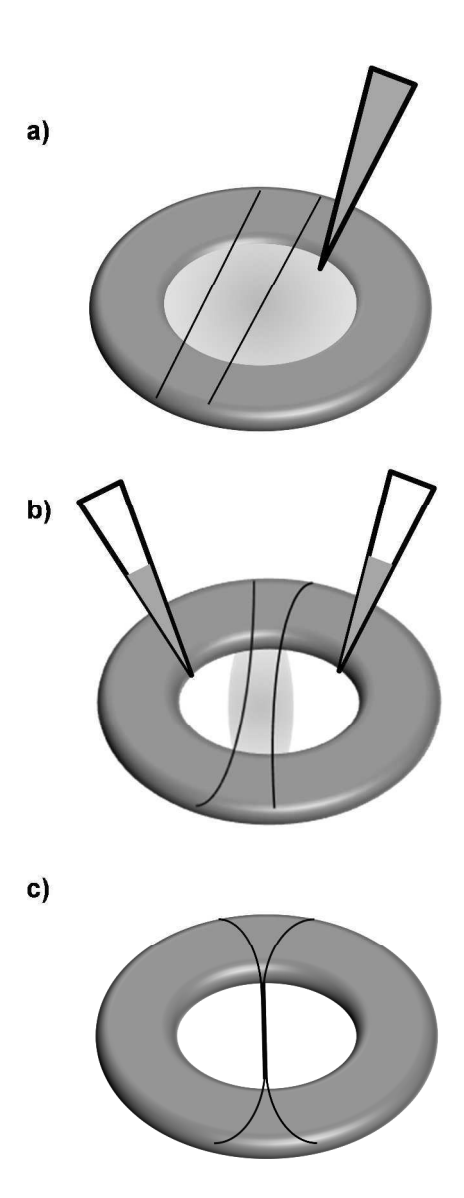


Figure 2. Addition of the general MMP inhibitor GM6001 to MCF10A and MCF10AT cells does not induce cell spreading. Neither addition of 12  $\mu$ M GM6001 (A,B) or the negative control N-t-butoxycarbonyl-L-leucyl-L-tryptophan methylamide (C,D) impacts the culture of MCF10A cells on tissue culture plastic or Ubx fibers. Addition of GM6001 (E,F) but not the negative control N-t-butoxycarbonyl-L-leucyl-L-tryptophan methylamide (G,H) induces MCF10AT cells to adopt a granular morphology on both tissue culture plastic and Ubx fibers.

